ARTICLE

A passive portable microfluidic blood-plasma separator for simultaneous determination of direct and indirect ABO/Rh blood typing

Received 00th January 20xx,
Accepted 00th January 20xx

DOI: 10.1039/x0xx00000x

Shadi Karimi,[a] Pouya Mehrdel [a] , Josep Farre Llados [a] and Jasmina Casals Terre [a]

Blood typing test is mandatory in any transfusion, organ transplant, and pregnancy situation. There is a lack of point-of-care (POC) blood typing that could perform both direct and indirect methods with a single droplet of whole blood. This study presents a new methodology to combine a passive microfluidic blood-plasma separator (BPS) and a blood typing detector for the very first time; leading to a stand-alone microchip which is capable of determining the blood group from both direct and indirect methods simultaneously. The proposed design separates blood cells from plasma by applying hydrodynamic forces imposed on them, which overcomes the clogging issue and consequently maximizes the volume of the extracted plasma. Axial migration effect across the main channel is responsible for collecting the plasma in plasma collector channels. The BPS novel design approached 12% yield of plasma with 100% purity in approximately 10 minutes. The portable BPS was designed and fabricated to perform the ABO/Rh blood tests based on the detection of agglutination in both antigens of RBCs (direct) and antibodies of plasma (indirect). The differences between agglutinated and non-agglutinated samples were distinguishable by the naked eye and also validated with particle analysis of microscopic pictures. The results of this passive BPS in ABO/Rh blood grouping verified the quality and quantity of the extracted plasma in practical applications.

Introduction

Blood is the most important body fluid in clinical diagnosis and also one of the simplest way to determine the internal performance of the human body. Blood is a mixture of various particles such as red blood cells (RBC), white blood cells (WBC) and platelets suspended in plasma. The plasma, which is around 55% of blood volume, contains various circulating biomarkers such as antibodies [1]. Different blood types exist due to the presence or absence of certain antigens on the surface of the RBCs and antibodies in the plasma. According to Landsteiner's law [2], if an antigen is present on patient RBCs, the corresponding antibody will not be present in the plasma under normal conditions. Non-compatible blood types would lead to an agglutination which is a visible clumping of RBCs with a particular antibody that indicates the presence of the specific corresponding antigen on the RBCs being tested. The absence of agglutination (a smooth stream of dilute RBCs) indicates that there is no specific corresponding antigen on the RBCs' surfaces. There is a standard category for blood grouping by differences in proteins available on RBCs' surfaces: type A (only A antigens), type B (only B antigens), type AB (both A and B antigens), type O (neither A nor B antigens). Additionally, the presence or absence of rhesus (Rh) factor (D) on the RBCs' surface divides each blood type into (Rh+) and (Rh-), respectively. A person with (Rh-) does not have Rh antigens naturally on their RBCs. This is the reason that a person with (Rh+) can receive blood from a person with (Rh-) without any problems [3]. Transfusion of non-compatible blood can result in severe health problems or sudden death. Currently, there are more than thirty genetic-based blood typing methods [4]. However, ABO system [2] and (Rh) system [5] which were discovered by Karl Landsteiner are the most important ones that are required for blood transfusions. Agglutinated blood cells can be detected using different assays with reliable sensitivity such as the traditional slide test, the tube test, the microplate method, gel column agglutination, and affinity column technology. These assays require special laboratory instruments operated by trained laboratory personnel, which increases the relative costs [6]. There are various modern technologies in ABO/Rh blood group typing as well, such as molecular blood typing, synthetic receptors, natural receptors, paper-based [7-10], emerging strategies, and blood test kits [6]. In emergency diagnosis, lateral flow assays based on a functionalized cellulose membrane are more common but less accurate. However, classical methods of blood typing still considered the most reliable and, therefore, adopted in clinical laboratories [3]. Recently the Micronics ABORhCard provided a rapid, credit card sized test for the simultaneous determination of an individual's ABO/Rh type from a finger prick sample of whole blood in 2 minutes [11]. A recent study of 26 fatal accidents due to the incompatibility of ABO/Rh showed that in 24% of the cases pre-transfusion bedside compatibility test (PBCT) was not done at

[a] *Mechanical Engineering Department - MicroTech Lab., Universitat Politècnica de Catalunya. Colom 7-11 08222 Terrassa Barcelona SPAIN*

the patient bedside, in 32% the PBCT was not done at all, and in 44% it was done on the transfused unit and not to the patient. Human mistakes related to blood typing are cited as the most frequent cause of problems in transfusion. Another study of two commercial POCT showed that the error occurred in 30% of the assays. The errors were attributed to the poor technique of the operator, device failure or incorrect interpretation [12]. Generally, there are two methods of ABO/Rh blood typing: Direct (forward) typing is based on a possible reaction of the antigens around the patients' RBCs while indirect (reverse) typing utilizes the reaction of natural antibodies from their plasma with identified RBCs. The results from performing these two methods simultaneously would significantly decrease the possible errors in blood typing. In another word, serum grouping (indirect method) used to confirm results obtained in RBC grouping (direct method). Conventional blood typing in most countries requires both direct and indirect methods. In order to perform the indirect method, the plasma needs to be extracted from blood since the existence of blood cells in plasma reduces the precision during analysis by inducing a great level of noise in the biochemical tests results. Therefore, blood-plasma separation is essential in blood analysis, disease diagnostics and other applications [13]. Centrifugation is generally accepted as the most conventional methods in blood-plasma separation despite its drawbacks such as bulky, heavy, and high cost, manipulation error and a large volume of blood sample requirement. Few researchers have addressed the problem of centrifugation with a Lab-On-Chip (LOC) devices (CD format [14-17]) which may result in rupture of blood cells and produce an unnecessary noise in the system. Microfluidic devices have been considered as an effective manner to overcome these limitations. The main advantages of LOC devices are smaller volume requirement of a blood sample, preanalytical standardization, low cost, highly accurate, rapid measurements, portability and decreased laboratory workload [18] [21]. Therefore, filtration is one of the proposed separation methods that could replace centrifugation [22]. Several solutions are available for miniaturizing a blood-plasma extraction such as paper-based format [23, 25] and microfluidic chip format. The procedure of blood-plasma separation in microfluidic devices is classified into two categories; Active and passive. Active methods rely on external energy for cell separation such as acoustic [26, 27], electrical [21] [28-30] and magnetic [1] [31, 32], while passive methods work autonomously without the aid of external energy [19]. Passive methods usually rely on capillary forces which include sedimentation [33-36], cell deviation [37, 38], and microfiltration [39-41]. Lenk et al. [42] integrated a wedge structure between a plasma filter and a channel with pores to provide a capillary contact. The input to the device was a 30-60 µl of whole blood which resulted in a 4 µl isolated plasma sample within 3 minutes. Maria et al.'s [35] microfluidic device could obtain 2 µl of plasma from 10 µl whole blood in 15 min with purification efficiency of 99.9%. The quality of plasma was validated by implementing a glucose detection test. Madadi et al. [39] had used cross-flow filtration and microposts when they achieved 0.1 µl of plasma from 5 µl of undiluted blood with a purity of 98% in 5 minutes and the extracted plasma was verified in TSH tests. Prabhakar et al. [43] designed a microfluidic channel with a combination of several effects such as Fahraeus effect, bifurcation law, cell-free region, centrifugal action, and constriction-expansion for blood-plasma separation. They achieved almost 100% of separation efficiency at a hematocrit level of 20 % but for undiluted blood, it was decreased to 80 %.

Most of the passive technics are suffered from clogging problem [19, 20]. This issue limits the amount of plasma available for analysis and therefore the type of test that can be implemented using microchip filtration. For instance, in a blood typing test, the sample has to be divided into five branches (three RBC outlets, and two plasma outlets) in order to test the ABO/Rh group for both direct and indirect method. Therefore, to perform the test, an adequate amount of plasma is needed. Previous works, such as Madadi et al. [39] achieved 100% purity but it resulted in a limited amount of plasma due to final clogging. This limitation was improved in Mohamadi et al. [44] but external forces were used. The presented design uses a novel shape of the top channel such as bubble-based corrugated side channels, and an expansion-contraction geometry to improve the amount of extracted plasma compared to Mohammadi's work which used an electric field to delay clogging. By the aid of a novel design of the top channel (dead-end zone) and cross-flow filtration, the proposed device achieves 6X the amount of extracted plasma from undiluted blood in less than 10 minutes compared to the previous design. The combination of the microfluidic BPS, that can maximize the volume of extracted plasma from a single droplet of whole blood, and a blood grouping detector concludes in developing a standalone ABO/Rh blood grouping chip in a single cartridge. This concept achieves fast, efficient, accurate, low cost and simple measurement of agglutination inside a passive microchip for both direct and indirect blood typing.

Design and method

Principle of design

The proposed BPS design is taking advantages of several aspects including fluid dynamics, separation science and technology, and blood rheology in order to maximize the volume of extracted plasma.

Figure 1 shows a schematic view of the BPS design, which is manufactured in two parts. The top part comprises a 25 µm depth main channel and two plasma collector channels with the same depth as Figure 1a illustrates. The geometry of the main channel improves blood plasma separation by increasing the perimeter of the channel compared to a simple straight channel. Longer perimeter leads to having more space for releasing plasma. Three different corrugated designs for the

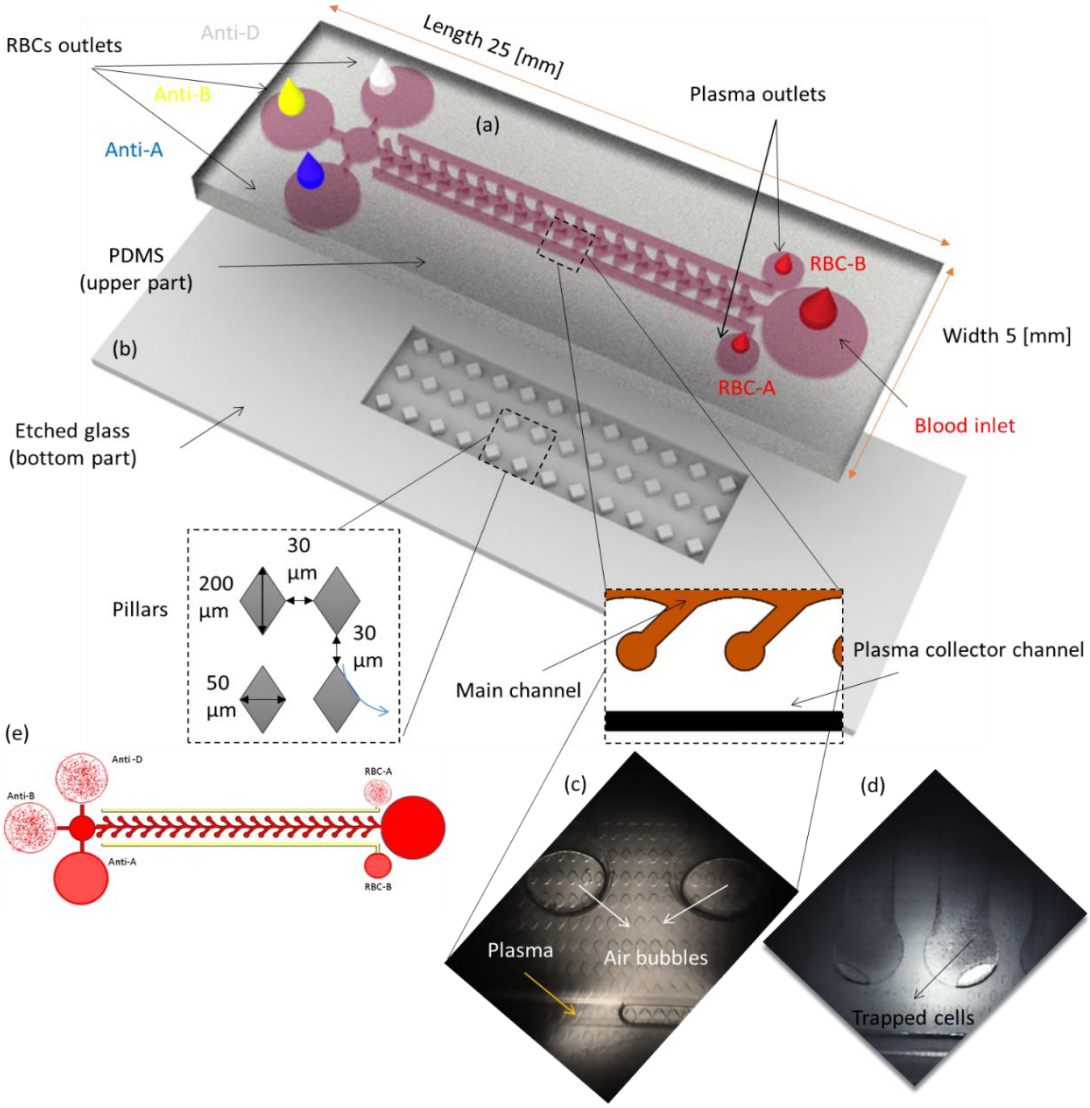

Figure 1 Schematic picture of the microchip and its dimensions (a) PDMS block that contains a main channel and two plasma collector channel (top part), (b) Etched glass with diamond pillars (bottom part), (c) microscopic picture of the creation of the air bubbles at the end of the side channels, (d) Initial process of trapping the particles during bubble disappearance, (e) schematic picture of an expected results of the ABO/Rh blood typing tests

main channel have been investigated and compared by the simulation to be selected for fabrication. The bottom part includes an array of pillars with diamond shape (Figure 1b) which has been shown [39] that has the minimum fluidic resistance compared to other shapes such as circle, elongated, pine and rectangular. These pillars not only filters RBCs but also paves the way for collecting the separated plasma in the top part by using plasma collector channels. To approach this goal, the maximum pillar thickness is chosen to be 1.8 µm which is less than minimum RBCs diameter (2µm) to prohibit escaping of the cells from the main channel and achieve 100% purity in the extracted plasma. A droplet of blood is infused into the inlet and the main channel is initially filled, afterward, plasma is extracted through the arrays of pillars and collected at the plasma collector channels via capillary forces. During this process, stagnation zones are generated at the dead-end branches and some RBCs are trapped there. The hydrodynamic effect of the dead-end branch length is investigated [44] by numerical analyses of different corrugated channels. The length of the side channels is chosen to be 400 µm due to the results that highlighted the advantages of using long dead-end branches which hydro-dynamically, captures RBCs in the dead- end zones [39]. Several constrictions are added in the main channel to generate a local flow acceleration and delay the RBCs clogging of the filtration area. Besides, a larger zone is placed at the end of each corrugated channel, creating initially a bubble of air in the PDMS part. Figure 1c shows the microscopic pictures of the microchannel right after a droplet of undiluted blood is introduced into the inlet. As soon as the blood is dropped to the channel, the separation process starts by capillary force. As it's shown in this figure bubbles are created in the large area of the corrugated channel. These bubbles vanish since PDMS is gas

permeable and consequently pulls the RBCs to the side channels. Hydrodynamic separation through the generation of stagnation zones keeps the RBCs at the end of branches. In fact, these bubbles work as a vacuum system to pull RBCs from the main channel to the sides. Hence, the clogging process at the main channel is postponed, leading to the extraction of a higher volume of plasma from a droplet of undiluted blood. In Figure 1d, the trapped cells after bubble disappearance have been presented which help to postpone the clogging process in the main channel. The main advantage of this design is the efficiency and maximization of the amount of obtained plasma from an initial sample by the elimination of external forces. In order to use the extracted plasma in an application, this BPS has been designed to be a blood type detector which is able to work with both direct and indirect methods, simultaneously.

The method used to determine blood type with the proposed device is based on the detection of agglutination via naked eye and the microscopic pictures to validate the visual results. Figure 1e illustrates the schematic of an expected formation of the positive and negative reaction of antigens and antibodies to determine the blood type from both methods. For instance, in Figure 1e a positive reaction with Anti-B and Anti-D and no reaction with Anti-A is depicted which indicates the blood type B-positive from the direct method. From the other hand, the results from the indirect method also indicate the blood type B, due to the reaction with Anti-A and no reaction with Anti-B. The results from the indirect method verify the results from the direct method.

Simulation

In order to study a better design for the main channel and divert more cells to the sides which postpones clogging process and consequently extract more plasma, three different designs with different corrugated shapes (Lopsided, Perpendicular, Misaligned-lopsided) are proposed. Figure 2 shows the schematics of the studied designs in a 2-D simulation. Fluid flow in a microchannel is assumed to be isothermal, incompressible, and laminar. Therefore, governed by the continuity, and momentum Navier–Stokes equations. These equations are expressed, respectively, as:

$$\boldsymbol{\nabla}.\vec{\boldsymbol{V}} = \mathbf{0} \qquad (1)$$

$$\frac{\partial \vec{V}}{\partial t} = -(\vec{V}.\boldsymbol{\nabla}).\vec{V} + \vartheta \boldsymbol{\nabla}^2 \vec{V} - \frac{1}{\rho}\boldsymbol{\nabla} p + \vec{f} \qquad (2)$$

Where $\vec{V}$ is velocity vector, ϑ is kinematic viscosity, ρ is density, p is pressure and $\vec{f}$ is body force such as gravity in this simulation.

The plasma flow for this simulation is considered as a Newtonian flow, its density and viscosity are set to 1025 [kg/m3] and 0.003 [kg.m-1.s-1]. The density of the particle is set to 1125 [kg/m3] since it is considered as RBC and its shape is assumed as a spherical with 5 µm in diameter. Commercial CFD-code software, ANSYS-workbench, FLUENT 19.2 (ANSYS, Inc.) is used to simulate the simplified blood flow inside a microchannel. Benefiting from Finite Volume approach, this solver solves the continuity and the momentum equations, at the steady-state case, at each control volume with respect to the physical properties of the introduced fluids, initial settings and boundary conditions (velocity inlet and pressure outlet). To carry out the numerical analysis, the solver is set to the SIMPLE scheme and for solving pressure and momentum modules the configuration of the software is set to the second-order method

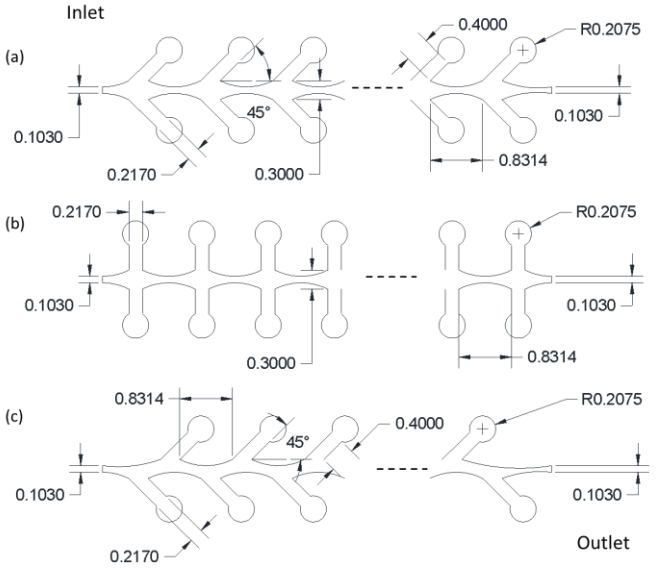

Figure 2 Overall dimensions of the models. All dimensions are in [mm]. Model (a), (b), and (c) are presented Lopsided, Perpendicular, and Misaligned-lopsided, respectively. The length of the channel in all three designs is 22 [mm]. Model (a) has 38 branches while model (b) has four more and model (c) has one less branch in the same length due to their specific geometry.

and second-order-upwind method, respectively.

The geometry meshed in ANSYS-workbench software. A grid independence study was done, based on four different mesh densities (low, medium, high and fine quality) while the residual was set to 10e-5 in all the cases. A quadratic mesh scheme with the minimum orthogonal quality of ~0.85 was allocated. The number of grid cells varied from 36,000 cells as a low-quality scheme to 932,000 cells as a fine scheme.

The mean interval size of each cell varied from 15 to 5 µm. Among those, the meshing configuration that provided 8 µm resulted in an acceptable answer accuracy. According to grid independency analysis, the mesh with cells 5 µm interval size cells showed no significant change in the results but the required calculation time was increased exponentially.

Methodology

The PBS device is placed under an optical upright microscope (Tucsen ISH500, Tokyo, Japan) with a micro inspection lens system (Optem zoom 125C with a broad 12.5:1 zoom range and a 20X objective). Whole blood samples are drawn from healthy volunteers at Mutua

Hospital in Terrassa and collected via 5 ml vacutainer collection tube which contains anti-coagulant (Ethylenediamine tetra-acetic acid) to postpone the sedimentation phenomena during the experimental setup. The samples are stored at 4 ºC temperature until usage to maximize the liveability of the cellular components and are gently mixed back and forward to prevent possible undesirable cells sedimentation prior to testing. All the experiments processed at the room temperature (20-25 °C). The results are observable with the naked eye. Although the microscopic pictures are taken to show the results with higher precision. An image processing is developed by an open source ImageJ software to analyze the particles by their population and verify the results from visual observation. To determine the purity of the extracted plasma, a rectangular area (200 µm × 400 µm) in the blood main channel is selected and compared with the same size area in the plasma collector channel. These areas are captured by microscope after the plasma collector channels are filled completely. The number of blood cells in these areas are counted by the particle analysis method of the ImageJ software. Eventually, purity is expressed by:

$$\text{Purity}\% = \left(1 - \left(\frac{\text{final cells density}}{\text{initial cells density}}\right)\right) * 100\% \qquad (3)$$

In order to qualify the amount of the separated plasma, the volume of the plasma in the lateral outlets which is measured by a disposal microsyringe (1 ml @Henke Sass Wolf Of America, Inc.), is compared to the volume of the droplet of injected blood. The result considers as the yield which is represented by:

$$\text{Yield}\% = \left(\frac{\text{output sample volume}}{\text{input sample volume}}\right) * 100\% \qquad (4)$$

On the other hand, three different antibodies; Anti-A in blue, Anti-B in yellow, and Anti-D with no color (DiaClon @BIO-RAD laboratories Inc. Hercules, California, United States) are added to each blood outlets to generate the possible agglutination for ABO/Rh blood typing from the direct method. Optimal agglutinate formation occurs when the amounts of antigen and antibody are in equivalent proportions. The prozone phenomenon occurs when either the antigen or the antibody is in excess which leads to false negative result [45]. In commercial kits (direct blood typing), the concentration of antibodies is optimal to create agglutination, however, in patient's serum the concentration of natural antibodies can change from patient to patient and the concentration may not be optimal to generate a strong agglutination in indirect blood typing. Therefore, detection of RBC agglutination due to natural incomplete (IgG) antibodies present in a patient's serum is more challenging. To perform the indirect blood typing method, two known blood samples (A and B) are prepared. These samples are added to the unknown extracted plasma. To achieve the optimal ratio, RBCs are slowly added to plasma on a separate laboratory glass. As more antigen is added, the reaction enters the equivalence zone, where both the optimal antigen-antibody interaction and maximal precipitation occur. If even more antigen was added, the amount of antigen would become excessive and actually cause the amount of precipitation to decline. After obtaining the optimum ratio between plasma and RBCs, a specified droplet of a known blood group is added on each plasma outlet at the end of the plasma collector channels, and well mixed. The criterion of agglutination is easily interpreted by the comparison between agglutinated with non-agglutinated cells. The type of blood is indicated from having or not having a reaction between antigens around the RBCs and antibodies in the plasma. For instance, agglutination occurs when anti-A is added to blood with A-antigen on its RBCs, revealing the blood type as A. The absence of this reaction means that the sample belongs to either blood type B or O. Finally, the results from ABO direct grouping method is validated with ABO indirect grouping method. To have a better observation of these changes caused by the addition of Anti-A, Anti-B, and anti-D to blood outlets and RBCs-A and RBCs-B to plasma outlets, each test repeated three times and each time a picture is taken from the outlet. There are 4 different blood samples in total to analyze. Each test needs three pictures for the direct method and two pictures for the indirect method. In case of having a reaction between antigens and corresponding antibody, agglutination occurs (cells stick together) and the number of unattached RBCs in that zone decreased significantly. A clear difference in the agglutinated and non-agglutinated reactions is observable for each blood type from both direct and indirect method. Whereas the agglutinated sample has less unattached particles than the non-agglutinated, fewer cells indicate the positive reaction.

Fabrication

The proposed device contains two parts; a polydimethylsiloxane (PDMS) part which comprises the blood transport main channel and the plasma collector channels (top part), and etched glass that has the array of pillars for plasma extraction (bottom part). These two parts are bonded via the oxygen-plasma method. A brief description of fabrication stages for each part is provided in Figure 3.

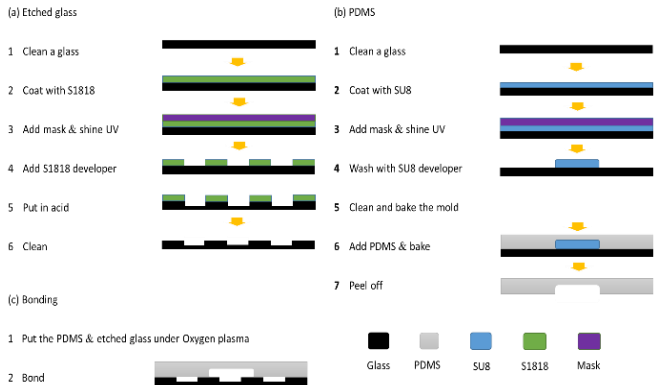

Figure 3 Fabrication process: (a) the standard wet etching process, (b) the conventional standard soft lithography procedure, (c) bonding process

Bottom part

The etched glass is fabricated according to the standard wet etching process, Figure 3a. The pattern for the etched part is

designed by AutoCAD 2018 and printed out with the high-quality printer on a UV-exposed double layer resist film to prepare the mask. The laboratory glass that is going to be used for etching is cleaned by the Piranha cleaning process. The spin coater is set to 2000 RPM in 30 s to reach 0.25 µm thickness. A layer of positive photoresist (MICROPOSIT S1818 @ DOW® chemical company, Midland, Michigan, United States) is coated on the cleaned glass in a darkroom. The pattern is printed on this layer with the help of UV light for 4.85 s. After the curing process on a hot plate, the rest of photoresist material is removed with the S1818 developer (MEGAPOSIT MF-24A @ DOW®) in 55 s. In order to etch 1.8 µm depth pillars, the glass substrate is immersed in HF acid (Hydrofluoric acid @ SIGMA-ALDRICH company, St. Louis, Missouri, United States) for 3 minutes. To remove the resist residues, acetone (@SIGMA-ALDRICH) in an ultrasonic bath is used then is rinsed with DI water and dried on a hotplate.

Top part

To form the microchannel on PDMS, the conventional standard soft lithography procedure is used which is illustrated in Figure 3b. A thick layer of epoxy based (SU-8 photoresist @ GERSTELTEC SÀRL from Pully, Switzerland) is coated on a cleaned laboratory glass in a dark room at 1080 RPM for 45 s to reach a uniform layer with 25 µm thickness. After 15 minutes' relaxation time, the coated substrate is soft-baked in two steps: 10 minutes at 65 °C and 60 minutes at 95 °C and is cooled down to the room temperature. The microchannel pattern is also designed by AutoCAD 2018 and printed out with the high-quality printer to make the mask. The pattern is printed on the coated substrate by UV exposure lamp for 8 seconds. After 10 minutes' delay time all the parts of uncured resist is washed with the SU-8 developer, PGMEA (Propylene glycol methyl ether acetate @GERSTELTEC SÀRL, Pully, Switzerland) for 4 minutes to obtain the master mold.

In order to create the PDMS part, a mixture of silicone elastomer base and its curing agent 10:1 (@SYLGARD 184, Dow Corning, Midland (MI) the United States) is prepared. The surface of the mold is covered by the vapor of Chlorotrimethylsilane (puriss., ≥99.0% (GC) @SIGMA-ALDRICH) under the hood to be able to peel off the PDMS from the mold easily. An open top aluminum box is made to place the mold. The mixture is poured on the mold and is heated for 1 hour at 80°C to bake the PDMS. The PDMS block which has microchannels pattern, simply is peeled off from the mold and cut into an acceptable piece and punched to create the orifices of inlet and outlets by using a biopsy micro puncher. As it is shown in Figure 3c the Oxygen-Plasma oven (Gambetti Vacuum Technology, Binasco (MI) Italy) is used to assist in irreversibly bonding the PDMS block to the etched glass. Oxygen plasma has to activate the surfaces of the PDMS and the etched glass that has to be bonded together. The plasma-time is set to 40 s and the power is set to 20 W, also the stabilization time is set on 10 s. After that, the reciprocal surfaces of both parts are activated so the PDMS is placed in contact with the glass and then the glass/PDMS structure is placed on a 75ºC hotplate for 5 minutes to increase the bonding strength.

Results and discussion

Numerical results

In order to optimize the design of the main channel three factors are considered; pressure drop, velocity, and particle concentration. Numerical simulation was performed at very low Reynolds number since blood is driven by capillary forces. The results showed that the Perpendicular design provides 2.52% less pressure drop than the Lopsided design while the Misaligned-lopsided design provides 58.33% less pressure drop compared to the Perpendicular design. Additionally, the evolution of Y velocity studied. In a horizontal line shown in Figure 5a from the inlet to the outlet of the main channel, parallel to the centerline but very close to the wall. Figure 5 shows the evolution of velocities in the Y direction as a function of the X position. The Y direction velocity in Misaligned-lopsided exceeds that of both Lopsided and Perpendicular designs by 187%. The results of this study indicate that Misaligned-lopsided pushes the particles towards the sides of the main channel with greater force delaying clogging effect through the channel.

Figure 4 illustrates the discrete phase model (DPM) concentration contours at the first branch after the inlet of each design. The increased concentration at a branch indicates more interactions and consequently more trapped particles at the side channels. The numerical simulation shows that since the flow is laminar, the flow lines expand following the main channel walls, and therefore, the channel walls' curvature affects the neighboring flow streams. Owing to the small scale of the microchannel, any changes in the direction and magnitude of the flow stream should not be neglected. The results from this study show that particle concentration is 56,70% more in the Misaligned-lopsided than Perpendicular designs and 22.42% than Lopsided design at the beginning of the branches. Therefore, the Misaligned-lopsided design has been chosen to be fabricated. It is fair to mention that since this simulation is in 2-D, there is a significant difference between numerical and experimental results. In fact, the channel has a bottom part (in the real case) that the flow can go to the sides which in the 2-D model is not considered, but since the bottom

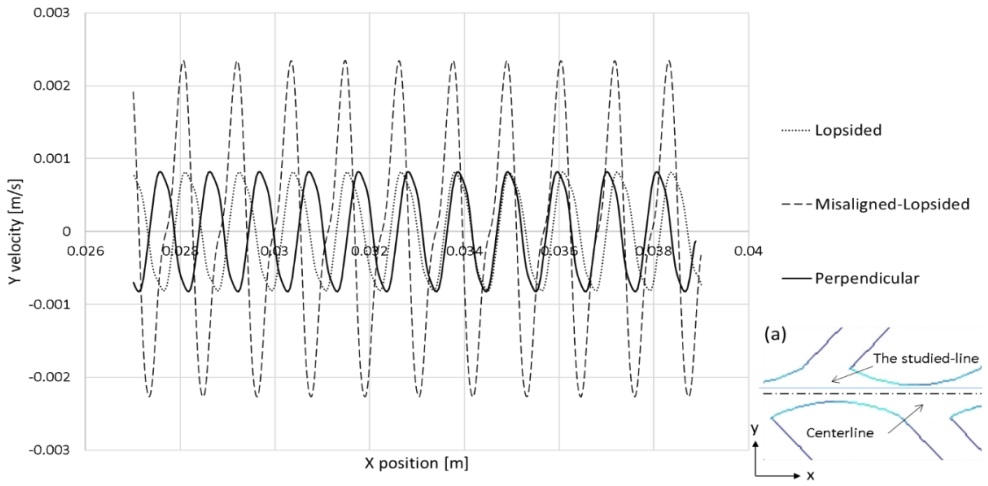

Figure 5 Comparison of velocity in Y direction on a horizontal line near side channels at each design (a) The studied line position in the main channel.

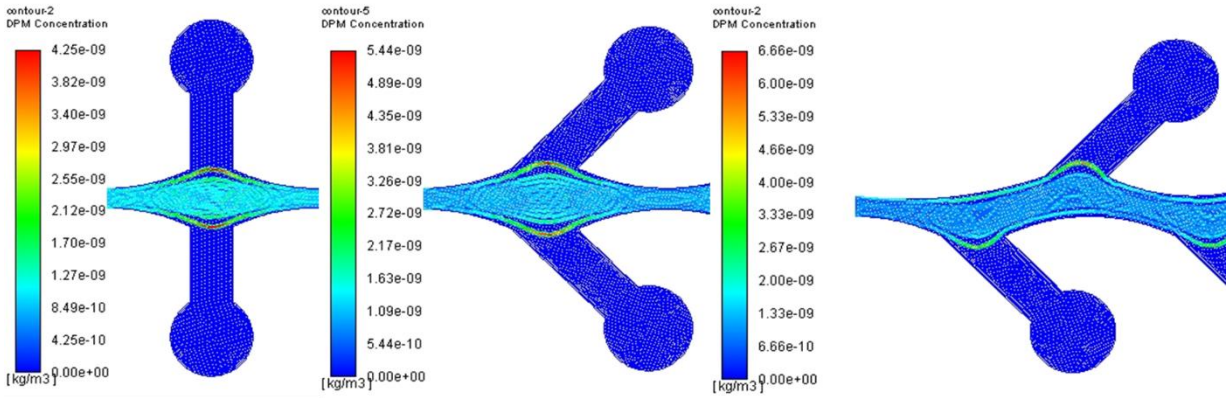

Figure 4 Comparison of DPM concentration at each branch (a) Perpendicular design (b) Lopsided design (c) Misaligned-lopsided design

part for all these three cases are the same so this study is performed to choose the best design for the top part to be fabricated.

BPS results

Three different devices were fabricated according to the methodology and a 50 µl droplet of undiluted blood was used for conducting the test. Table 1 shows the amount of extracted plasma from each device with respect to their extraction-time. According to the results, the plasma collector channels are completely filled in around 10 min. The amount of extracted plasma from each collected channel is 3±0.3 µl. Based on the Equation (4), this device has a 12% yield.

Table 1. Specification of the plasma outlet geometry and the extracted plasma.

Tests	Volume [µl]	Time [min]
1st	5.7	9
2nd	6.5	12
3rd	6	10

Figure 6 shows the evolution of the blood from the main channel to the plasma collector channel. Figure 6a illustrates the main channel filling process which trapped the cells completely in the sides thanks to the novel design and bubble disappearance vacuuming technic. Figure 6b depicts the cell-free region at the main channel after 5 minutes which allows the injection of even more blood that results in extracting a larger amount of plasma. Figure 6c and d show the area used to evaluate the purity of plasma. After directly counting the number of blood cells in these areas, it has been confirmed that final blood cells in the plasma collector channels are zero. According to the Equation (3), the efficiency of purity obtained 100% which means all the RBCs are trapped in the main channel and no cell penetrates to the plasma collector channels. The excellent purity of the extracted plasma is one of the significant advantages of this device. The other remarkable property is its separation efficiency without requiring any dilution of a blood sample. The major superiority of this device compared to the simple straight main channel [39] is that the amount of extracted plasma from the corrugated main channel has been raised by 6 folds. This enhancement is due to the increase of extraction area since the corrugated design is 2.5 times larger

than a simple straight channel. Besides, the existence of bubbles at the end of the corrugated design delays the clogging process.

Since the amount of extracted plasma is adequate to be divided into several outlets, multiple detections can be applied to this device. Therefore, the BPS device is used to implement direct and indirect blood typing.

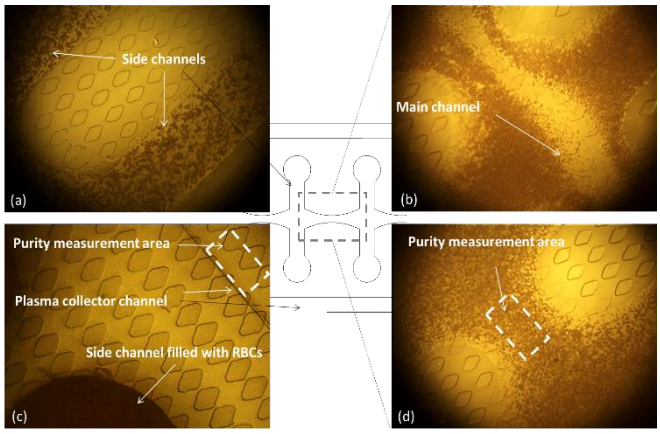

Figure 6 (a) Trapping of RBCs in the side channels, (b) Pulling RBCs to the side channels , (c) The area of purity measurement at the plasma collector channel, (d) Purity measurement area at the main channel after 10 minutes

The comparison of the BPS system that we have presented in here with the other passive BPS designs is prepared in Table 2. All of them work with undiluted blood sample. Our design has several potential as a POC device. It is a self-driven microfluidic system which doesn't need any pumps or external forces. The system can be integrated by introducing different reagents in order to apply other tests. Having the possibility of integration of different reagents in either blood outlet or plasma outlet leads us to multiplex this system with an ABO/Rh blood typing test. In this case three blood outlets will identify the blood type from direct method and two outlets from plasma collector channels is just suitable to validate the results of the blood type from the indirect method

Table 2. Comparison of latest passive BPS which works with whole blood

Name	Volume injected	Purity	Yield	Time
Maria et al. [35]	10	99.9	20	15
Hojat et al. [39]	5	98	2	3-5
Lenk et al. [42]	30-60	-	13	3
Park et al. [36]	15	100	0.2	-
This work	50	100	12	10

Application to blood typing

The proposed BPS is designed to perform the blood typing with both direct and indirect methods, simultaneously. In order to validate the appropriate mixing ratio for direct method, three different amount of IgM antibodies; 1, 2, and 3 µl are added on three different laboratory glasses and mixed with 3 µl of blood, prior to the test implementation. The most detectable agglutination belongs to the glass with an equal amount of antibody and blood (3 µl of each) as it is shown in Figure 7a which is in agreement with the results presented in other studies [45]. Due to the strong bindings between IgM antibodies and antigens of the direct method, the differences in agglutination behavior of the three mixture compositions are easily distinguishable by the naked eye. The glass number one in Figure 7a shows the reaction between unknown blood and Anti-A while no reaction is observed with Anti-B and Anti-D, which clarifies the type of blood to be A (Rh-). Whereas the results from the glass number two shows the indication of blood type B (Rh-), due to the absence of any reaction with Anti-A and D.

For indirect blood typing, the ratio of added RBCs is also optimized. Taking into account the fact that the human blood group antibodies are mostly IgG and therefore, the agglutination is not easily visible by naked eye. Since the confirmation of possible reaction is easier with higher contrast between agglutinated and non-agglutinated samples, the differences of positive and negative reactions are investigated.

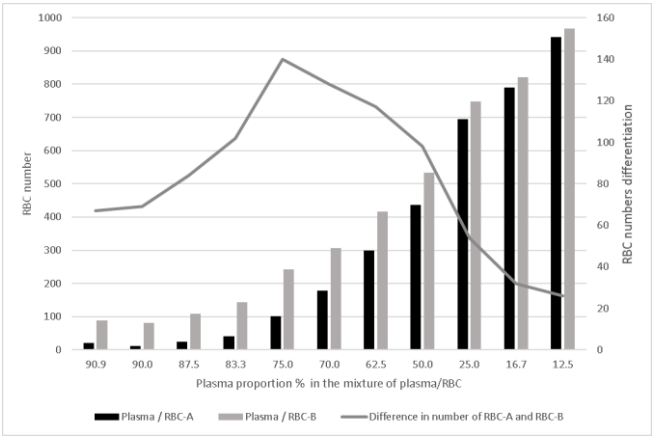

Figure 8. Experimental results of optimizing the plasma/RBC ratio

Figure 8 shows positive and negative reaction differences of various plasma/RBC ratios, in order to keep the required volume of the plasma as minimum as possible while maximizing the difference between positive and negative reactions. For this reason, the number of unattached cells for each positive and negative reactions are counted by ImageJ software and compared with all other sample ratios. According to Figure 8, 75% plasma ratio is selected to achieve the highest value of

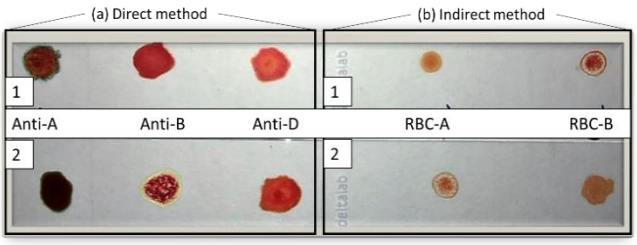

Figure 7 preliminary experiments on the glass for direct and indirect method

differentiation between a positive and negative reaction. The agglutinated and non-agglutinated patterns at this mixing ratio are detectable by naked eye as presented in Figure 7b. In this figure, 1 µl RBC is added to 3 µl plasma. The existence of agglutination in a mixture of an unknown plasma sample and RBC-A indicates blood type B and vice versa. In the plasma extracted from type B blood, there are anti-A while in plasma from type A, there are Anti-B. The results from the indirect method are indicating the blood type A on the glass number one (reaction between plasma and RBC-B) and B on the glass number two (reaction between plasma and RBC-A), which is in agreement with the results from the direct method.

At this point, the microfluidic BPS is used to perform all these separated tests in a single standalone device. A droplet of 3 µl from each antibody is dropped on the corresponding RBC´s outlet to be mixed with the unknown blood sample.

Figure 9 shows the real picture of microchip that is used to analyze blood typing. The photographs are taken at the same time as the microscopic measurements. Three different pictures are taken from these three outlets under the microscope. This figure shows the blood type A (Rh-) since there are positive reactions with Anti-A, but no reaction with Anti-B and Anti-D.

After this short procedure, the plasma is extracted and ready to be mixed with two known blood samples from group A and B. One droplet of 1 µl from each RBC-A and RBC-B samples are added to the outlets of plasma collector channels, to see the possible reaction with the antibodies in the extracted plasma after getting mixed. Two pictures are captured from these outlets as well and compared with the pictures from the direct method to verify the blood type. Representative agglutination patterns from the microscopic pictures that are captured from the outlets are depicted also in Figure 9. The agglutination of the aforementioned cells will allow the determination of the blood type from the natural antibodies of the patient's plasma. Figure 9a shows the agglutination with Anti-A and in Figure 9b and c no reaction with Anti-D or Anti-B is seen. Which verifies a person with blood type A (Rh-). In Figure 9e the positive reaction of RBCs-B and antibodies that caused an agglutination is visible and Figure 9d indicates that there is no reaction between RBCs-A and a particular antibody available in plasma, which determines the blood type A and validates the result from direct method.

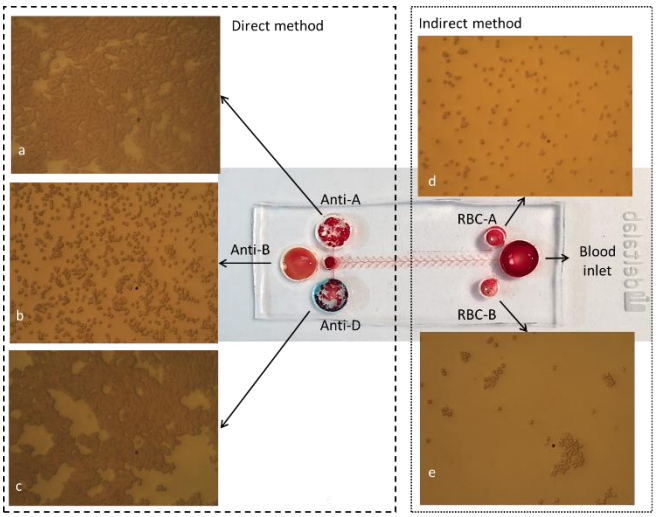

Figure 9 The real device. The microscopic pictures of reaction of blood sample with different antibodies; (a) Anti-A, (b) Anti-B, (c) Anti-D & the visible clumping of RBCs with a particular antibody (d) RBCs-A, (e) RBCs-B, which mixed with unknown extracted plasma.

The ABO/Rh blood typing test is conducted using A+, A-, B+, B-, AB+, AB-, O+, and O- blood types. The ImageJ calculated the number of unattached particles at each outlet. All the blood types that are shown in Figure 10, contains three bars for the direct methods and two bars for indirect. The differences are significant. The direct method compares the mixture of blood cells and anti-A, B, and D by their particle numbers, while in indirect method the particle numbers are representatives of the comparison of the mixture of plasma and RBC-A and RBC-B. The number of unattached particles from the direct method is higher since 3µl of the whole blood sample is mixed with antibody while for the indirect method just a droplet of 1µl of RBCs is used. In these graphs for the indirect method if the number of counted cells are less than 100, it is considered as a positive reaction and for direct method the positive reaction is for less than 300 cells. For instance, the blood type A (Rh-) has a reaction with Anti-A and Anti-D and no reaction with Anti-B, from the direct method, and since there is no Anti-A in its plasma, there is no reaction with plasma A that verifies the results from direct method.

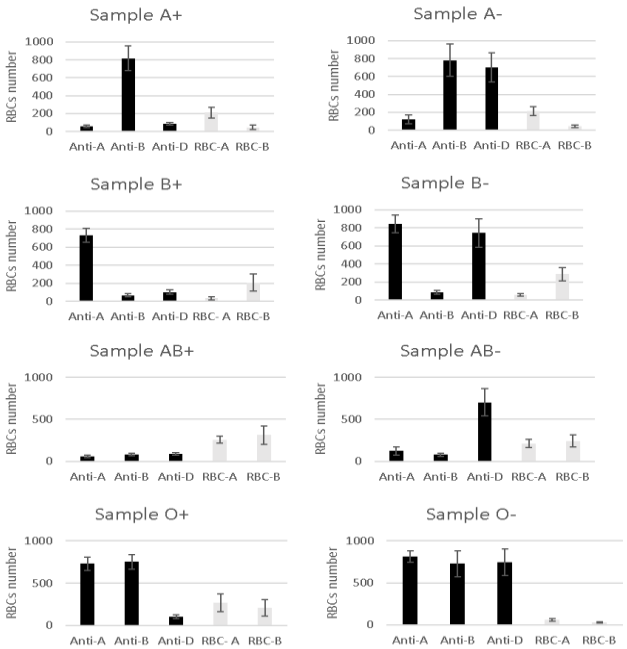

Figure 10 Comparison of the number of RBCs in a mixture of blood group A (Rh+), A (Rh-), B (Rh+)and B (Rh-) AB (Rh+), AB(Rh-), O(Rh+), O(Rh-) with Antibody A, B and D in black; and also in a mixture of plasma and RBC A and B in grey, to show the positive or negative reactions from both direct and indirect methods.

Tolerance for hematocrit validation

The hematocrit (HCT), is a blood test that measures the volume percentage of red blood cells in blood. Hematocrit can vary from the determining factors of the number of red blood cells. These factors can be from the age and sex of the subject. The measurement depends on the number and size of red bloods cells. It is normally 40.7% to 50.3% for men and 36.1% to 44.3% for women. Considering on-site blood typing, the hematocrit level of the tested sample is usually unknown, and this can influence the results. Thus the method should perform variable values of hematocrit. To this end the tolerance of the number of particles for three different dilution ratio was tested.

Three different hematocrit level of a blood sample are prepared which their RBC volume is constitute between 20% to 50%. In order to establish the validity of our system as a blood typing detector, the influence of haematocrit ratio has been analysed. Figure 11 shows the numbers of single free RBCs for all the samples which are mixture of each blood type (A, B, AB, and O) with Anti-A and Anti-B separately. ImageJ is used for this analyzation. This device couldn't generate a reliable result for a sample with higher than 55% of hematocrit ratio, presumably due to the high viscosity which confront the capillary force and result in fast drying and clogging in the channel. However, all four types of blood showed similar behaviour for three diluted ratios of 20, 35 and 50%. Blood type O has no reaction with neither Anti-A nor Anti-B while blood type AB reacted with both antibodies.

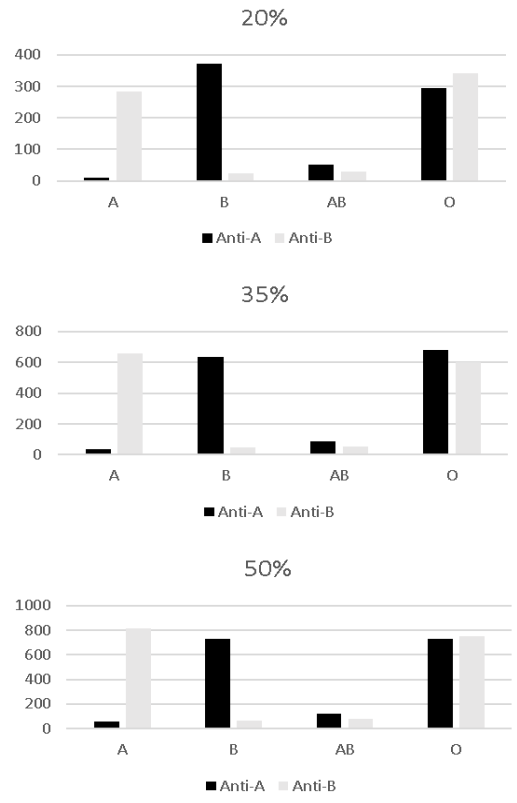

Figure 11 Effect of various hematocrit values on blood group determination. The hematocrit of blood was artificially set to three indicated value in case of blood sample from four different blood groups then tested in microfluidic channel system where the two outlets were functionalized by Anti-A and Anti-B group antibodies. Anti-A is indicated in black and Anti-B in grey.

It should be noted that the limitation of this study is that Anti-A and Anti-B used are colored, in the same manner as general diagnostic reagents used for manual ABO/Rh blood typing, the anti-A is blue and the anti-B is yellow in color. These colors could possibly affect the visual blood type detection with naked eye, but not with particle analysis. Our hemagglutination detection method demonstrated the capability to deal with such challenging cases. We consider that the microscopic sensor-based hemagglutination detection is more sensitive and accurate than a visual test but it could be explored in further research on integration of this method with a photonic detection system. Additionally, in order to create a stand-alone POC blood typing test, the measurement of the agglutination should be quantified. Further work could lead to efficient biomarker detection [46].

Conclusions

A novel microfluidic channel with dead-end branches at each side was designed, fabricated and validated through ABO/Rh blood typing tests. Three different microfluidic channel designs were simulated using finite elements methods. The appropriate design achieved a better RBC trapping in the side channels. By the help of dead-end zone part at the end of each branch of corrugated channels, the clogging process was postponed, therefore the volume of extracted plasma was maximized. The experiment has required only a single droplet (50 µl) of whole blood without the need of any external forces or pre analytical steps. A volume of 6 µl plasma was successfully extracted in about 10 min with the highest purity level (100%). The microfluidic device was closed except for the inlet and outlet ports, protecting the reaction from environmental interference. From the outcome of this investigation it is possible to conclude that the BPS design has potential to be used in several applications as a POC device. The availability of multiple channels in this design has proved suitable for blood typing tests by introducing different reagents with small volumes. This passive microfluidic ABO/Rh blood typing system was designed for simultaneous detection of direct typing tests and indirect typing tests by naked eye. The eye-catching accuracy of results was also validated by microscopic evaluations. This device is self-driven, low cost, simple, portable, accurate, and fast for blood typing which leads to numerous applications in hospitals, clinics, and local laboratories.

Conflicts of interest

There are no conflicts of interest to declare.

Acknowledgements

This research was funded by Spanish Ministry of Economy and Competitively, grant numbers CTQ2017-84966-C2-1-R and CTQ2016-77936-R.

References

1 P. Kim, Eh. Ong, KH. Li, YJ. Yoon, SH. Ng, K. Puttachat. *Low-cost, disposable microfluidics device for blood plasma extraction using continuously alternating paramagnetic and diamagnetic capture modes.* Biomicrofluidics. 2016 Mar 17;10(2):024110.

2 K. Landsteiner. *Zur Kenntnis der antifermentativen lytischen and agglutinierendenWirkung des Blutserums and der lymph. Zentralbl. Bakteriol. Parasit. Infekt*. 1900, 27, 357–362.

3 M. Adnan, L.D. Franz. *Blood Group Typing: From Classical Strategies to the Application of Synthetic Antibodies Generated by Molecular Imprinting*. Sensors 2016, 16, 51; doi:10.3390/s16010051.

4 Z. Liu, M. Liu, T. Mercado, O. Illoh, R. Davey. *Extended blood group molecular typing and next-generation sequencing. Transfus.* Med. Rev. 2014, 28, 177–186. [CrossRef] [PubMed]

5 K. Landsteiner. *Ueber Agglutinationserscheinungen normalen menschlichen Blutes*. Wien. Klin. Wochenschr. 1901, 14, 1132–1134.

6 W. Malomgré, B. Neumeister. *Recent and future trends in blood group typing. Analytical and bioanalytical chemistry.* 2009 Mar 1;393(5):1443-51.

7 M. Li, WL. Then, L. Li, W. Shen. *Based device for rapid typing of secondary human blood groups*. Analytical and bioanalytical chemistry. 2014 Jan 1;406(3):669-77.

8 J. Noiphung, K. Talalak, I. Hongwarittorrn, N. Pupinyo, P. Thirabowonkitphithan, W. Laiwattanapaisal. *A novel paper-based assay for the simultaneous determination of Rh typing and forward and reverse ABO blood groups.* Biosensors and Bioelectronics. 2015 May 15; 67:485-9.

9 WL. Then, M. Li, H. McLiesh, W. Shen, G. Garnier. *The detection of blood group phenotypes using paper diagnostics*. Vox sanguinis. 2015 Feb 1;108(2):186-96.

10 M. Al-Tamimi, W. Shen, R. Zeineddine, H. Tran, G. Garnier. *Validation of paper-based assay for rapid blood typing.* Analytical chemistry. 2012 Jan 9;84(3):1661-8.

11 https://www.micronics.net/products/diagnostic-products/immunohematology

12 H. Maxime, C. Myriam, B. Arnaud. *Red blood cell agglutination for blood typing within passive microfluidic biochips.* High-throughput MDPI 2018, (10).

13 S. Tripathi, YB. Kumar, A. Agrawal, A. Prabhakar, SS. Joshi. *Microdevice for plasma separation from whole human blood using bio-physical and geometrical effects*. Scientific reports. 2016 Jun 9; 6:26749.

14 BS Lee, JN Lee, JM Park, JG Lee, S Kim, YK Cho, C. Ko. *A fully automated immunoassay from whole blood on a disc.* Lab on a Chip. 2009;9(11):1548-55.

15 S. Haeberle, T. Brenner, R. Zengerle, J. Ducrée. *Centrifugal extraction of plasma from whole blood on a rotating disk.* Lab on a Chip. 2006;6(6):776-81.

16 CT. Schembri, V. Ostoich, PJ. Lingane, TL Burd, SN. Buhl. *Portable simultaneous multiple analyte whole-blood analyzer for point-of-care testing. Clinical chemistry*. 1992 Sep 1;38(9):1665-70.

17 M. Amasia, M. Madou. *Large-volume centrifugal microfluidic device for blood plasma separation.* Bioanalysis. 2010 Oct;2(10):1701-10.

18 N. Xiang, Z Ni. *High-throughput blood cell focusing and plasma isolation using spiral inertial microfluidic devices.* Biomedical microdevices. 2015 Dec 1;17(6):110.

19 MS. Maria, TS. Chandra, AK. Sen. *Capillary flow-driven blood plasma separation and on-chip analyte detection in microfluidic devices.* Microfluidics and Nanofluidics. 2017 Apr 1;21(4):72.

20 L. Xu, H. Lee, MV. Brasil Pinheiro, P. Schneider, D. Jetta, KW Oh. *Phaseguide-assisted blood separation microfluidic device for point-of-care applications*. Biomicrofluidics. 2015 Jan 21;9(1):014106.

21 WS. Mielczarek, EA. Obaje, TT. Bachmann, M. Kersaudy-Kerhoas. *Microfluidic blood plasma separation for medical diagnostics: is it worth it?.* Lab on a Chip. 2016;16(18):3441-8.

22 M. Kersaudy-Kerhoas, E. Sollier. *Micro-scale blood plasma separation: from acoustophoresis to egg-beaters.* Lab on a Chip. 2013;13(17):3323-46.

23 E. Carrilho, AW. Martinez, GM. Whitesides. *Understanding wax printing: a simple micropatterning process for paper-based microfluidics.* Analytical chemistry. 2009 Jul 15;81(16):7091-5.

24 X. Li, DR. Ballerini, W. Shen. *A perspective on paper-based microfluidics: current status and future trends.* Biomicrofluidics. 2012 Mar 2;6(1):011301.

25 T. Songjaroen, W. Dungchai, O. Chailapakul, CS. Henry, W. Laiwattanapaisal. *Blood separation on microfluidic paper-based analytical devices.* Lab on a Chip. 2012;12(18):3392-8.

26 A. Lenshof, C. Magnusson, T. Laurell. *Acoustofluidics 8: Applications of acoustophoresis in continuous flow microsystems.* Lab on a Chip. 2012;12(7):1210-23.

27 M. Wiklund. *Acoustofluidics 12: Biocompatibility and cell viability in microfluidic acoustic resonators.* Lab on a Chip. 2012;12(11):2018-28.

28 CM. Das, F. Becker, S. Vernon, J. Noshari, C. Joyce, PR. Gascoyne. *Dielectrophoretic segregation of different human cell types on microscope slides.* Analytical chemistry. 2005 May 1;77(9):2708-19.

29 Y. Nakashima, S. Hata, T. Yasuda. *Blood plasma separation and extraction from a minute amount of blood using dielectrophoretic and capillary forces.* Sensors and Actuators B: Chemical. 2010 Mar 4;145(1):561-9.

30 H. Jiang, X. Weng, CH. Chon, X. Wu, D. Li. *A microfluidic chip for blood plasma separation using electro-osmotic flow control.* Journal of Micromechanics and Microengineering. 2011 Jul 11;21(8):085019.

31 AL. Rodríguez-Villarreal, MD. Tarn, LA. Madden, JB. Lutz, J. Greenman, J. Samitier, N. Pamme. *Flow focussing of particles and cells based on their intrinsic properties using a simple diamagnetic repulsion setup.* Lab on a Chip. 2011;11(7):1240-8.

32 CW. Yung, J. Fiering, AJ. Mueller, DE. Ingber. *Micromagnetic–microfluidic blood cleansing device.* Lab on a Chip. 2009;9(9):1171-7.

33 XB. Zhang, ZQ. Wu, K. Wang, J. Zhu, JJ. Xu, XH. Xia, HY. Chen. *Gravitational sedimentation induced blood delamination for continuous plasma separation on a microfluidics chip.* Analytical chemistry. 2012 Mar 29;84(8):3780-6.

34 CC. Wu, LZ Hong, CT. Ou. *Blood cell-free plasma separated from blood samples with a cascading weir-type microfilter using dead-end filtration.* Journal of Medical and Biological Engineering. 2012 Jan 1;32(3):163-8.

35 MS Maria, PE. Rakesh, TS. Chandra, AK. Sen. *Capillary flow-driven microfluidic device with wettability gradient and sedimentation effects for blood plasma separation.* Scientific reports. 2017 Mar 3; 7:43457.

36 S. Park, R. Shabani, M. Schumacher, YS. Kim, YM. Bae, KH. Lee, HJ. Cho. *On-chip whole blood plasma separator based on microfiltration, sedimentation and wetting contrast*. Microsystem Technologies. 2016 Aug 1;22(8):2077-85.

37 V. Doyeux, T. Podgorski, S. Peponas, M. Ismail, G. Coupier. *Spheres in the vicinity of a bifurcation: elucidating the*

Zweifach–Fung effect. Journal of Fluid Mechanics. 2011 May; 674:359-88.

38 TM. Geislinger, B. Eggart, S. Braunmüller, L. Schmid, T. Franke. *Separation of blood cells using hydrodynamic lift.* Applied Physics Letters. 2012 Apr 30;100(18):183701.

39 H. Madadi, J. Casals-Terré, M. Mohammadi. *Self-driven filter-based blood plasma separator microfluidic chip for point-of-care testing.* Biofabrication. 2015 May 22;7(2):025007.

40 C. Li, C. Liu, Z. Xu, J. Li. *The dual role of deposited microbead plug (DMBP): A blood filter and a conjugate reagent carrier toward point-of-care microfluidic immunoassay.* Talanta. 2012 Aug 15; 97:376-81.

41 KH. Chung, YH. Choi, JH. Yang, CW. Park, WJ. Kim, CS. Ah, GY. Sung. *Magnetically-actuated blood filter unit attachable to pre-made biochips.* Lab on a Chip. 2012;12(18):3272-6.

42 G. Lenk, J. Hansson J, W. van der Wijngaart, G. Stemme, N. Roxhed. *Capillary driven and volume-metred blood-plasma separation.* In2015 Transducers-2015 18th International Conference on Solid-State Sensors, Actuators and Microsystems (TRANSDUCERS) 2015 Jun 21 (pp. 335-338). IEEE.

43 A. Prabhakar, YB. Kumar, S. Tripathi, A. Agrawal. *A novel, compact and efficient microchannel arrangement with multiple hydrodynamic effects for blood plasma separation*. Microfluidics and Nanofluidics. 2015 May 1;18(5-6):995-1006.

44 M. Mohammadi, H. Madadi, J. Casals-Terré, J. Sellarès. *Hydrodynamic and direct-current insulator-based dielectrophoresis (H-DC-iDEP) microfluidic blood plasma separation.* Analytical and bioanalytical chemistry. 2015 Jun 1;407(16):4733-44.

45 *https://microbeonline.com/immunology-note/*

46 *Huet M, Cubizolles M, Buhot A. Real time observation and automated measurement of red blood cells agglutination inside a passive microfluidic biochip containing embedded reagents. Biosensors and Bioelectronics. 2017 Jul 15;93:110-7.*